



The effective beam width of a partially coherent rectangular multi-Gaussian Schell-model vortex beam propagating in a turbulent plasma

H. O. AL-Nadary¹, Abdu A. Alkelly¹, M. A. H. Khaled¹, Labiba F. Hassan^{1,*}

¹ Physics Department, Faculty of Science, Sana'a University, Sana'a, Yemen

* Corresponding author: labibahassan71@gmail.com

ARTICLE INFO

Article history:

Received: July 12, 2023

Accepted: August 1, 2023

Published: August, 2023

KEYWORDS

1. Effective beam width
2. Partially coherent
3. Rectangular multi-Gaussian Schell-model
4. Turbulent plasma

ABSTRACT

Based on the derived analytical formulae for the optical intensity and effective beam width of a partially coherent rectangular multi-Gaussian Schell-model (RMGSM) vortex beam, we analyzed the evolution of the effective beam width of a partially coherent RMGSM vortex beam propagating in an anisotropic turbulent plasma using numerical examples. The numerical results demonstrated that the effective beam widths in the x and y directions were similar. In studies on the influences of the source parameters, one can see that an RMGSM vortex beam with a larger topological charge l and beam waist w_0 or a smaller correlation coefficient σ evolves into a beam with a larger effective beam width. However, the influence of beam order was not evident. In addition, numerical examples proved that the effective beam width increases with increasing propagation distance and refractive index fluctuation variance $\langle n_1^2 \rangle$ or decreasing anisotropy parameter ξ_x , outer scale L_0 , and inner scale l_0 . This study's results will be beneficial for applications in free-space optical communications.

CONTENTS

1. Introduction
2. Theoretical Model
3. Results and Discussion
4. Conclusion
5. References

1. Introduction:

The phenomenon of laser beams propagating through atmospheric turbulence has garnered significant **interest** in recent years due to its applications in optical communication and remote sensing [1, 2]. In reality, a hypersonic plasma sheath forms around an aircraft as it pierces the Earth's atmosphere at an extremely high speed (hypersonic) because the gas

environment around the hypersonic aircraft rubs against the aircraft's body [3, 4]. The communication properties between vehicles and radar can be significantly affected by the existence of anisotropic turbulent plasma sheaths around aircraft. This can impede communication and cause break-in connections in certain cases [5, 6]. The propagation of various laser beams in

anisotropic turbulent plasma has received significant attention over the past decades [7-11]. There has been much interest in the propagation of optical beams with phase singularities in turbulent atmospheres. Gbur and Tyson proposed that in optical communications, the topological charge may be used as an information carrier by looking at how vortex beams, such as Laguerre-Gaussian beams, propagate through weak-to-strong atmospheric turbulence [12]. According to Wang *et al.*, atmospheric turbulence has less impact on the spreading of partially coherent vortex beams than on partially coherent nonvortex beams [13]. Recent advancements in laser technology have led to the introduction of novel rectangular beams produced by multi-Gaussian sources. This beam is called a rectangular multi-Gaussian Schell-model (RMGSM) vortex beam. Free-space propagation characteristics were also investigated. The results showed that the RMGSM vortex beam maintained its central dark core over short propagation distances. Subsequently, it eventually transforms into a rectangular flat-topped beam with increasing propagation distance [14]. To the best of our knowledge, no research has been published on the effect of turbulent plasma on the effective beam width of RMGSM vortex beams.

In this study, we first derive an analytical formula for the effective beam widths of an RMGSM vortex beam through a turbulent plasma. Second, we examine the effect of various beam and plasma parameters on the effective beam widths for an RMGSM vortex beam using numerical simulation. Finally, conclusions of this study are presented.

2. Theoretical Model

The cross-spectral density of the RMGSM vortex beam at the plane $z = 0$ of the Cartesian system can be written as [14, 15]:

$$\begin{aligned}
 W(\mathbf{r}'_1, \mathbf{r}'_2, 0) &= \frac{1}{C_1 C_2} (x'_1 + iy'_1)^l (x'_2 - iy'_2)^l \\
 &\times \exp\left(-\frac{x'^2_1 + y'^2_1}{w_0^2} - \frac{x'^2_2 + y'^2_2}{w_0^2}\right) \\
 &\times \sum_{n_1=1}^{N_1} \binom{N_1}{n_1} \frac{(-1)^{n_1-1}}{n_1} \exp\left[-\frac{(x'_2 - x'_1)^2}{2 n_1 \sigma^2}\right] \\
 &\times \sum_{n_2=1}^{N_2} \binom{N_2}{n_2} \frac{(-1)^{n_2-1}}{n_2} \exp\left[-\frac{(y'_2 - y'_1)^2}{2 n_2 \sigma^2}\right],
 \end{aligned}
 \tag{1}$$

where:

$$\begin{aligned}
 C_1 &= \sum_{n_1=1}^{N_1} \binom{N_1}{n_1} \frac{(-1)^{n_1-1}}{n_1} \\
 C_2 &= \sum_{n_2=1}^{N_2} \binom{N_2}{n_2} \frac{(-1)^{n_2-1}}{n_2}
 \end{aligned}
 \tag{2}$$

where $\mathbf{r}'_i = (x'_i, y'_i)$ is the position coordinate in the plane $z = 0$ ($i = 1, 2$), l is the topological charge, w_0 is the beam waist of a Gaussian beam, N_1 and N_2 are the numbers of Gaussian functions that can control the flat part of the x and y components, respectively, σ is the correlation coefficient.

Effective beam width is a useful parameter for describing the spreading characteristics of a beam. The effective beam width of the partially coherent RMGSM vortex beam through the turbulent plasma in the s -direction at plane z is defined as [16]

$$w_s(z) = \sqrt{2 \frac{\iint s^2 \langle I(\mathbf{r}, z) \rangle dx dy}{\iint \langle I(\mathbf{r}, z) \rangle dx dy}} \quad (s = x, \text{ or } y)
 \tag{3}$$

where I is the optical intensity, which depends on variables x , y , and z , and $\langle . \rangle$ denotes the ensemble average. In accordance with the expanded Huygens-Fresnel integral formula, the optical intensity of a partially coherent laser vortex beam propagating through turbulent anisotropic plasma is given by [17]

$$\begin{aligned}
 I(\mathbf{r}, z) = & \\
 & \times \left(\frac{k}{2\pi z}\right)^2 \iint d^2\mathbf{r}'_1 d^2\mathbf{r}'_2 W(\mathbf{r}'_1, \mathbf{r}'_2, 0) \\
 & \times \exp\left\{-\frac{ik}{2z} [(\mathbf{r} - \mathbf{r}'_1)^2 - (\mathbf{r} - \mathbf{r}'_2)^2]\right\} \\
 & \times \langle \exp[\psi^*(\mathbf{r}'_1, \mathbf{r}, z) + \psi(\mathbf{r}'_2, \mathbf{r}, z)] \rangle, \quad (4)
 \end{aligned}$$

where $k = 2\pi/\lambda$ is the wave number, λ is the wavelength, and ψ denotes the complex phase turbulence due to the random medium, which can be expressed as [9, 18]

$$\begin{aligned}
 \langle \exp[\psi^*(\mathbf{r}'_1, \mathbf{r}, z) + \psi(\mathbf{r}'_2, \mathbf{r}, z)] \rangle \cong \\
 \exp\{-D(z) [(\mathbf{r}'_2 - \mathbf{r}'_1)^2]\}. \quad (5)
 \end{aligned}$$

where $D(z)$ is the wave-structure function. If an anisotropic turbulent plasma is employed, the wave structure function is as follow [19]

$$\begin{aligned}
 D(z) = & \frac{32 z \pi^3 k^2 a_1 L_0^2 (m_1 - 1) \langle n_1^2 \rangle (\xi_x^2 + \xi_y^2)}{3 \xi_x^3 \xi_y^3} \\
 & \times \left(\frac{1}{100 L_0^2}\right)^4 \Gamma(4) U\left(4, 5 - m_1, \frac{1}{100 L_0^2 \kappa_0}\right), \quad (6)
 \end{aligned}$$

where $a_1 = 475 (\kappa_0)^{2m_1}$, $\kappa_0 = (2\pi/l_0)^{m_1 - 0.7}$, l_0 is the inner scale, $m_1 = 4 - d$ is a constant, d is the fractal dimension for fully developed turbulence, $d = 2.6$, and $m_1 = 1.4$. L_0 is the outer scale (satisfy $L_0/l_0 = R_e^{3/4}$, $R_e = 5 \times 10^5$ is the Reynolds number), $\langle n_1^2 \rangle$ is the refractive index fluctuation variance, ξ_x and ξ_y are anisotropy parameters, $\Gamma(\cdot)$ is the Gamma function and $U(\cdot)$ is a confluent hypergeometric function of the second type. Substituting Eqs. (1), (5), and (6) into Eq. ((4), and applying the following integral and expressions [20, 21]:

$$(x + iy)^n = \sum_{t=0}^n \frac{n!}{t!(n-t)!} x^{n-t} (iy)^t, \quad (7)$$

$$H_n(x) = \sum_{s=0}^{n/2} \frac{(-1)^s n!}{s!(n-2s)!} (2x)^{n-2s}, \quad (8)$$

$$\begin{aligned}
 & \int_{-\infty}^{+\infty} x^t \exp(-px^2 - 2qx) dx = t! \sqrt{\frac{\pi}{2}} \left(\frac{q}{p}\right)^t \\
 & \times \exp\left(\frac{q^2}{p}\right) \sum_{k=0}^{t/2} \frac{1}{k! (t-2k)!} \left(\frac{p}{4q^2}\right)^k, \quad (9)
 \end{aligned}$$

The optical intensity of an RMGSM vortex beam propagating in turbulent plasma at plane z is obtained as follows:

$$\begin{aligned}
 I(\mathbf{r}, z) & \\
 & = \frac{k^2}{4\pi^2 z^2} \frac{1}{C_1 C_2} \sum_{n_1=1}^{N_1} \binom{N_1}{n_1} \frac{(-1)^{n_1-1}}{n_1} \\
 & \times \sum_{n_2=1}^{N_2} \binom{N_2}{n_2} \frac{(-1)^{n_2-1}}{n_2} \sum_{t_1=0}^l \frac{l! i^{t_1}}{t_1! (l-t_1)!} \\
 & \times \sum_{t_2=0}^l \frac{l! (-i)^{t_2}}{t_2! (l-t_2)!} I(x, z) I(y, z), \quad (10)
 \end{aligned}$$

where:

$$\begin{aligned}
 I(x, z) & \\
 & = (l-t_1)! \sqrt{\frac{\pi}{a_x}} \left(\frac{1}{a_x}\right)^{l-t_1} \exp\left[\frac{1}{a_x} \left(\frac{ik}{2z} x\right)^2\right] \\
 & \times \sum_{d=0}^{\frac{l-t_1}{2}} \frac{1}{d! (l-t_1-2d)!} \left(\frac{a_x}{4}\right)^d \\
 & \times \sum_{e=0}^{l-t_1-2d} \frac{(l-t_1-2d)!}{e! (l-t_1-2d-e)!} \left(\frac{ik}{2z} x\right)^{l-t_1-2d-e} \\
 & \times \left[\frac{1}{2n_1 \sigma^2} + D(z)\right]^e \sqrt{\frac{\pi}{b_x}} 2^{-l+t_2-e} i^{l-t_2+e} \\
 & \times \exp\left(\frac{c_x^2}{b_x}\right) \left(\frac{1}{b_x}\right)^{0.5(l-t_2+e)} H_{l-t_2+e}\left(-i \frac{c_x}{\sqrt{b_x}}\right) \\
 & , \quad (11)
 \end{aligned}$$

$$\begin{aligned}
 I(y, z) &= (t_1)! \sqrt{\frac{\pi}{a_y}} \left(\frac{1}{a_y}\right)^{t_1} \exp\left[\frac{1}{a_y} \left(\frac{ik}{2z} y\right)^2\right] \\
 &\times \sum_{d=0}^{\frac{t_1}{2}} \frac{1}{d! (t_1 - 2d)!} \left(\frac{a_y}{4}\right)^d \\
 &\times \sum_{e=0}^{t_1 - 2d} \frac{(t_1 - 2d)!}{e! (t_1 - 2d - e)!} \left(\frac{ik}{2z} y\right)^{t_1 - 2d - e} \\
 &\times \left[\frac{1}{2 n_2 \sigma^2} + D(z)\right]^e \sqrt{\frac{\pi}{b_y}} 2^{-(t_2+e)} i^{t_2+e} \\
 &\times \exp\left(\frac{c_y^2}{b_y}\right) \left(\frac{1}{b_y}\right)^{0.5(t_2+e)} H_{t_2+e}\left(-i \frac{c_y}{\sqrt{b_y}}\right)
 \end{aligned} \tag{12}$$

with

$$a_x = \frac{1}{w_0^2} + \frac{1}{2 n_1 \sigma^2} + D(z) + \frac{ik}{2z}, \tag{13}$$

$$a_y = \frac{1}{w_0^2} + \frac{1}{2 n_2 \sigma^2} + D(z) + \frac{ik}{2z}, \tag{14}$$

$$\begin{aligned}
 b_x &= \frac{1}{w_0^2} + \frac{1}{2 n_1 \sigma^2} + D(z) - \frac{ik}{2z} \\
 &- \frac{1}{a_x} \left[\frac{1}{2n_1\sigma^2} + D(z)\right]^2,
 \end{aligned} \tag{15}$$

$$\begin{aligned}
 b_y &= \frac{1}{w_0^2} + \frac{1}{2 n_2 \sigma^2} + D(z) - \frac{ik}{2z} \\
 &- \frac{1}{a_y} \left[\frac{1}{2n_2\sigma^2} + D(z)\right]^2,
 \end{aligned} \tag{16}$$

$$c_x = \frac{1}{a_x} \left[\frac{1}{2n_1\sigma^2} + D(z)\right] \frac{ik}{2z} x - \frac{ik}{2z} x, \tag{17}$$

$$c_y = \frac{1}{a_y} \left[\frac{1}{2n_2\sigma^2} + D(z)\right] \frac{ik}{2z} y - \frac{ik}{2z} y, \tag{18}$$

On substituting Eq. (10) into Eq. (3) , after integral calculations, the effective beam width of a partially coherent RMGSM vortex beam in turbulent plasma is obtained as follows:

$$w_s(z) = \sqrt{2 \frac{A(s,2)}{A(r,0)}}, \tag{19}$$

with:

$$\begin{aligned}
 A(x, 2) &= \sum_{n_1=1}^{N_1} \binom{N_1}{n_1} \frac{(-1)^{n_1-1}}{n_1} \\
 &\times \sum_{n_2=1}^{N_2} \binom{N_2}{n_2} \frac{(-1)^{n_2-1}}{n_2} \sum_{t_1=0}^l \frac{l! i^{t_1}}{t_1! (l - t_1)!} \\
 &\times \sum_{t_2=0}^l \frac{l! (-i)^{t_2}}{t_2! (l - t_2)!} E(x, 2) E(y, 0),
 \end{aligned} \tag{20}$$

$$\begin{aligned}
 A(y, 2) &= \sum_{n_1=1}^{N_1} \binom{N_1}{n_1} \frac{(-1)^{n_1-1}}{n_1} \\
 &\times \sum_{n_2=1}^{N_2} \binom{N_2}{n_2} \frac{(-1)^{n_2-1}}{n_2} \sum_{t_1=0}^l \frac{l! i^{t_1}}{t_1! (l - t_1)!} \\
 &\times \sum_{t_2=0}^l \frac{l! (-i)^{t_2}}{t_2! (l - t_2)!} E(x, 0) E(y, 2),
 \end{aligned} \tag{21}$$

$$\begin{aligned}
 (r, 0) &= \sum_{n_1=1}^{N_1} \binom{N_1}{n_1} \frac{(-1)^{n_1-1}}{n_1} \\
 &\times \sum_{n_2=1}^{N_2} \binom{N_2}{n_2} \frac{(-1)^{n_2-1}}{n_2} \sum_{t_1=0}^l \frac{l! i^{t_1}}{t_1! (l - t_1)!} \\
 &\times \sum_{t_2=0}^l \frac{l! (-i)^{t_2}}{t_2! (l - t_2)!} E(x, 0) E(y, 0),
 \end{aligned} \tag{22}$$

where:

$$\begin{aligned}
 E(x, 0) &= (l - t_1)! \sqrt{\frac{\pi}{a_x}} \left(\frac{1}{a_x}\right)^{l-t_1} \\
 &\times \sum_{d=0}^{\frac{l-t_1}{2}} \frac{1}{d! (l - t_1 - 2d)!} \left(\frac{a_x}{4}\right)^d \\
 &\times \sum_{e=0}^{l-t_1-2d} \frac{(l - t_1 - 2d)!}{e! (l - t_1 - 2d - e)!} \left(\frac{ik}{2z}\right)^{l-t_1-2d-e} \\
 &\times \left[\frac{1}{2n_1\sigma^2} + D(z)\right]^e (l - t_2 + e)! \sqrt{\frac{\pi}{b_x}} \\
 &\times \left(\frac{1}{b_x}\right)^{l-t_2+e} \sum_{f=0}^{\frac{l-t_2+e}{2}} \frac{1}{f! (l - t_2 + e - 2f)!} \left(\frac{b_x}{4}\right)^f \\
 &\times \left[\frac{1}{a_x} \left(\frac{1}{2n_1\sigma^2} + D(z)\right) \frac{ik}{2z} - \frac{ik}{2z}\right]^{l-t_2+e-2f} \\
 &\times \sqrt{\frac{\pi}{q_x}} 2^{-2l+t_1+t_2+2d+2f} i^{2l-t_1-t_2-2d-2f} \\
 &\times \left(\frac{1}{q_x}\right)^{\frac{(2l-t_1-t_2-2d-2f)}{2}} H_{2l-t_1-t_2-2d-2f}(0)
 \end{aligned} \tag{23}$$

$$\begin{aligned}
 E(x, 2) &= (l - t_1)! \sqrt{\frac{\pi}{a_x}} \left(\frac{1}{a_x}\right)^{l-t_1} \\
 &\times \sum_{d=0}^{\frac{l-t_1}{2}} \frac{1}{d! (l - t_1 - 2d)!} \left(\frac{a_x}{4}\right)^d \\
 &\times \sum_{e=0}^{l-t_1-2d} \frac{(l - t_1 - 2d)!}{e! (l - t_1 - 2d - e)!} \left(\frac{ik}{2z}\right)^{l-t_1-2d-e} \\
 &\times \left[\frac{1}{2n_1\sigma^2} + D(z)\right]^e (l - t_2 + e)! \sqrt{\frac{\pi}{b_x}} \\
 &\times \left(\frac{1}{b_x}\right)^{l-t_2+e} \sum_{f=0}^{\frac{l-t_2+e}{2}} \frac{1}{f! (l - t_2 + e - 2f)!} \left(\frac{b_x}{4}\right)^f \\
 &\times \left[\frac{1}{a_x} \left(\frac{1}{2n_1\sigma^2} + D(z)\right) \frac{ik}{2z} - \frac{ik}{2z}\right]^{l-t_2+e-2f} \\
 &\times \sqrt{\frac{\pi}{q_x}} 2^{-2l+t_1+t_2+2d+2f+2} i^{2l-t_1-t_2-2d-2f+2} \\
 &\times \left(\frac{1}{q_x}\right)^{\frac{(2l-t_1-t_2-2d-2f+2)}{2}} H_{2l-t_1-t_2-2d-2f+2}(0)
 \end{aligned} \tag{24}$$

$$\begin{aligned}
 E(y, 0) &= (t_1)! \sqrt{\frac{\pi}{a_y}} \left(\frac{1}{a_y}\right)^{t_1} \sum_{d=0}^{\frac{t_1}{2}} \frac{1}{d! (t_1 - 2d)!} \left(\frac{a_y}{4}\right)^d \\
 &\times \sum_{e=0}^{t_1-2d} \frac{(t_1 - 2d)!}{e! (t_1 - 2d - e)!} \left(\frac{ik}{2z}\right)^{t_1-2d-e} \\
 &\times \left[\frac{1}{2n_2\sigma^2} + D(z)\right]^e (t_2 + e)! \sqrt{\frac{\pi}{b_y}} \left(\frac{1}{b_y}\right)^{t_2+e} \\
 &\times \sum_{f=0}^{\frac{t_2+e}{2}} \frac{1}{f! (t_2 + e - 2f)!} \left(\frac{b_y}{4}\right)^f \\
 &\times \left[\frac{1}{a_y} \left(\frac{1}{2n_2\sigma^2} + D(z)\right) \frac{ik}{2z} - \frac{ik}{2z}\right]^{t_2+e-2f} \\
 &\times \sqrt{\frac{\pi}{q_y}} 2^{-(t_1+t_2-2d-2f)} i^{t_1+t_2-2d-2f} \\
 &\times \left(\frac{1}{q_y}\right)^{0.5(t_1+t_2-2d-2f)} H_{t_1+t_2-2d-2f}(0)
 \end{aligned} \tag{25}$$

$$\begin{aligned}
 E(y, 2) &= (t_1)! \sqrt{\frac{\pi}{a_y}} \left(\frac{1}{a_y}\right)^{t_1} \sum_{d=0}^{\frac{t_1}{2}} \frac{1}{d! (t_1 - 2d)!} \left(\frac{a_y}{4}\right)^d \\
 &\times \sum_{e=0}^{t_1-2d} \frac{(t_1 - 2d)!}{e! (t_1 - 2d - e)!} \left(\frac{ik}{2z}\right)^{t_1-2d-e} \\
 &\times \left[\frac{1}{2n_2\sigma^2} + D(z)\right]^e (t_2 + e)! \sqrt{\frac{\pi}{b_y}} \left(\frac{1}{b_y}\right)^{t_2+e} \\
 &\times \sum_{f=0}^{\frac{t_2+e}{2}} \frac{1}{f! (t_2 + e - 2f)!} \left(\frac{b_y}{4}\right)^f \\
 &\times \left[\frac{1}{a_y} \left(\frac{1}{2n_2\sigma^2} + D(z)\right) \frac{ik}{2z} - \frac{ik}{2z}\right]^{t_2+e-2f} \\
 &\times \sqrt{\frac{\pi}{q_y}} 2^{-(t_1+t_2-2d-2f+2)} i^{t_1+t_2-2d-2f+2} \\
 &\times \left(\frac{1}{q_y}\right)^{0.5(t_1+t_2-2d-2f+2)} H_{t_1+t_2-2d-2f+2}(0)
 \end{aligned} \tag{26}$$

with:

$$\begin{aligned}
 q_x &= \frac{1}{a_x} \left(\frac{k}{2z}\right)^2 + \frac{1}{b_x} \left[\frac{1}{a_x} \left(\frac{1}{2n_1\sigma^2} + D(z)\right) \frac{k}{2z} - \frac{k}{2z}\right]^2 \\
 q_y &= \frac{1}{a_y} \left(\frac{k}{2z}\right)^2 + \frac{1}{b_y} \left[\frac{1}{a_y} \left(\frac{1}{2n_2\sigma^2} + D(z)\right) \frac{k}{2z} - \frac{k}{2z}\right]^2
 \end{aligned} \tag{27}$$

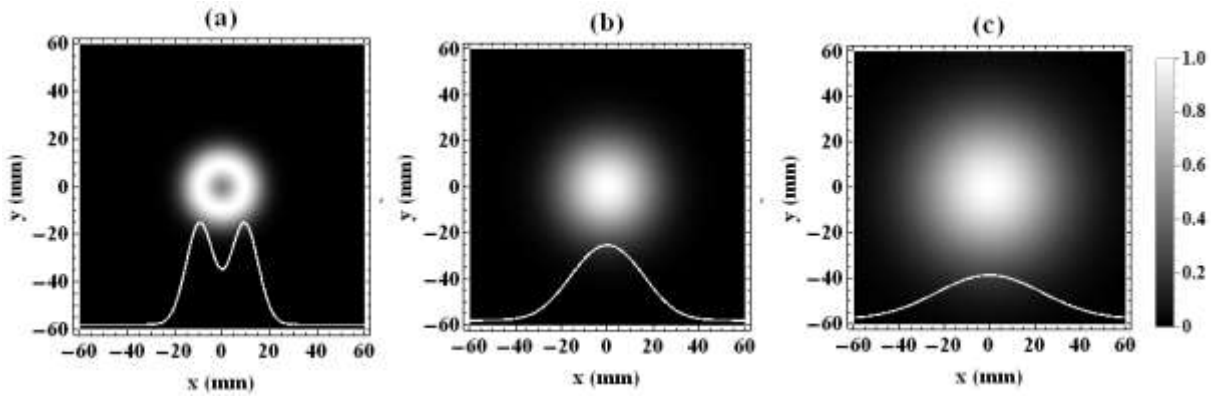


Figure 1 : Intensity distribution of partially coherent RMGSM vortex beam with different propagation distances z in turbulent plasma: (a) $z = 1\text{ m}$, (b) $z = 2\text{ m}$, and (c) $z = 3\text{ m}$.

3. Results and discussion

In this section, we study the effects of various beam and plasma parameters on the effective beam width of a partially coherent RMGSM vortex beam propagated in anisotropic turbulent plasma using a set of numerical examples. The following parameters are supposing, unless stated otherwise: the beam parameters are: $N_1 = N_2 = 3$, $l = 2$, $\sigma = 1\text{mm}$, $w_0 = 1\text{cm}$, $\lambda = 1550\text{nm}$ and the turbulent plasma parameters are $\xi_x = 2$, $\xi_y = 1$, $\langle n_1^2 \rangle = 0.73 \times 10^{-20}$, $l_0 = 5 \times 10^{-6}\text{m}$, $L_0 = 0.1\text{m}$ (which satisfied the conditions in Ref. [19]).

Figure 1 shows the evolution of the intensity distributions of a partially coherent RMGSM vortex beam with $l = 2$ in turbulent plasma, where the intensity distribution is plotted for different propagation distances z (1, 2, 3) m. As can be seen, the intensity distributions of a partially coherent RMGSM vortex beam propagating through turbulent plasma undergo several stages of evolution. A central dark core exists in the $z = 0$ plane. At $z = 2\text{m}$, an intensity profile with a central dip was observed. Ultimately, it transforms into a Gaussian shape

as the propagation distance increases to $z = 3\text{ m}$. As shown in Figure1 , the effective beam widths in the x and y directions follow a similar variational rule. Thus, the following analysis is only shown in the x -direction $w_x(z)$.

Figure 2 illustrates the changes in the effective beam width of the partially coherent RMGSM vortex beam for different beam parameter values (beam order $N_1 = N_2$, topological charge l , correlation coefficient σ , and beam waist w_0) versus propagation distance z in the turbulent plasma. From the curves in Figure 2(a), it can be observed that $w_x(z)$ gradually increased with propagation. In addition, the partially coherent RMGSM vortex beams with different $N_1 = N_2$ values (5, 10, and 15) exhibit almost the same spreading features (see Figure 2(a)); thus, the effects of $N_1 = N_2$ on $w_x(z)$ can be ignored. From Figure 2(b), it can be observed that $w_x(z)$ gradually increased with propagation. When the propagation distance is from 0 to 1m , the effective beam width shows little change. However, this change was significant when the propagation distance was $z > 1\text{m}$. In addition, we found that $w_x(z)$ increased with increasing l . Figure 2(c) shows $w_x(z)$ of the partially coherent RMGSM vortex beam for different values of σ

(0.1 mm, 0.4 mm, and ∞). Figure 2(c) shows that $w_x(z)$ gradually increases with propagation. However, a partially coherent RMGSM vortex

beam with a smaller σ has a larger $w_x(z)$ value as the propagation distance z increases. Thus, a larger

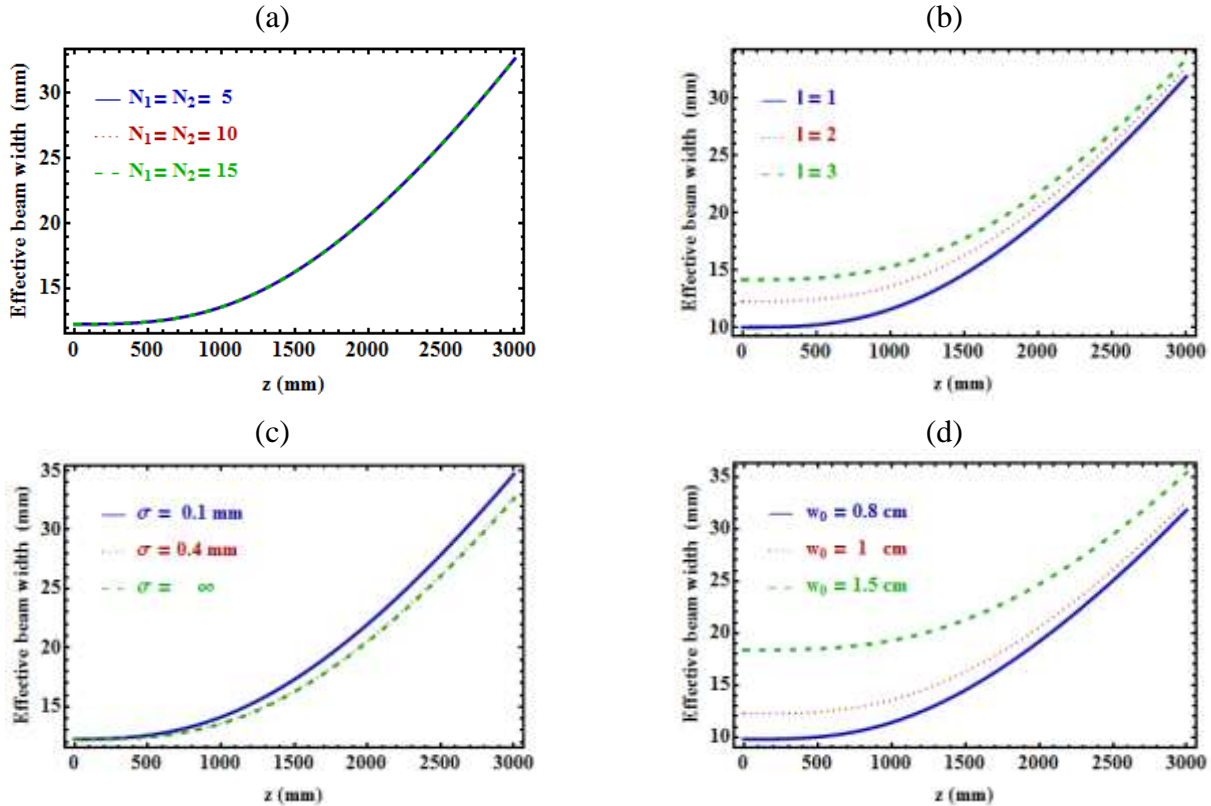


Figure 2: Effective beam width of the partially coherent RMGSM vortex beam versus the propagation distance z in the turbulent plasma for the different : (a) beam order $N_1 = N_2$, (b) topological charge l , (c) correlation coefficient σ , and (d) beam waist w_0 .

correlation coefficient, the lower the influence of turbulence on the spreading of beam width. Figure 2(d) shows $w_x(z)$ of the partially coherent RMGSM vortex beam for different w_0 (0.8 cm, 1, and 1.5 cm) in the turbulent plasma. From Figure 2(d), it can be observed that $w_x(z)$ gradually increased with propagation. In addition, the effective beam width increased with an increase in w_0 ; this indicates that the beam with a smaller beam waist was less affected by the turbulent plasma.

Figure 3 illustrates the changes in the effective beam width of the partially coherent RMGSM

vortex beam for different values of the plasma parameters (anisotropy parameter ξ_x , refractive index fluctuation variance $\langle n_1^2 \rangle$, outer scale L_0 , and inner scale l_0) versus the propagation distance z in the turbulent plasma. In Figure 3(a), we plotted $w_x(z)$ of the partially coherent RMGSM vortex beam for different values of ξ_x (1, 3, 6). It is evident from Figure 3(a) that the anisotropy parameter of the turbulent plasma significantly affects the spreading properties of the partially coherent RMGSM vortex beam. The partially coherent RMGSM vortex beam spread more rapidly as ξ_x decreased.

Figure 3(b) plots $w_x(z)$ of the partially coherent RMGSM vortex beam for different values of $\langle n_1^2 \rangle$. From the curves in this figure, it can be observed that $w_x(z)$ gradually increased with propagation. The effective beam width also increases with an increase in turbulence strength $\langle n_1^2 \rangle$. In Figure 3(c) and 3(d), $w_x(z)$ of the partially coherent RMGSM vortex beam

propagating in the turbulent plasma is shown for different L_0 and l_0 , respectively. From Figure 3(c) and 3(d), it can be observed that all the curves gradually increase with propagation. In the far field, $w_x(z)$ decreased with increasing L_0 and l_0 . This means that, for turbulent plasma with larger values of L_0 and l_0 , its effect on the beam is less.

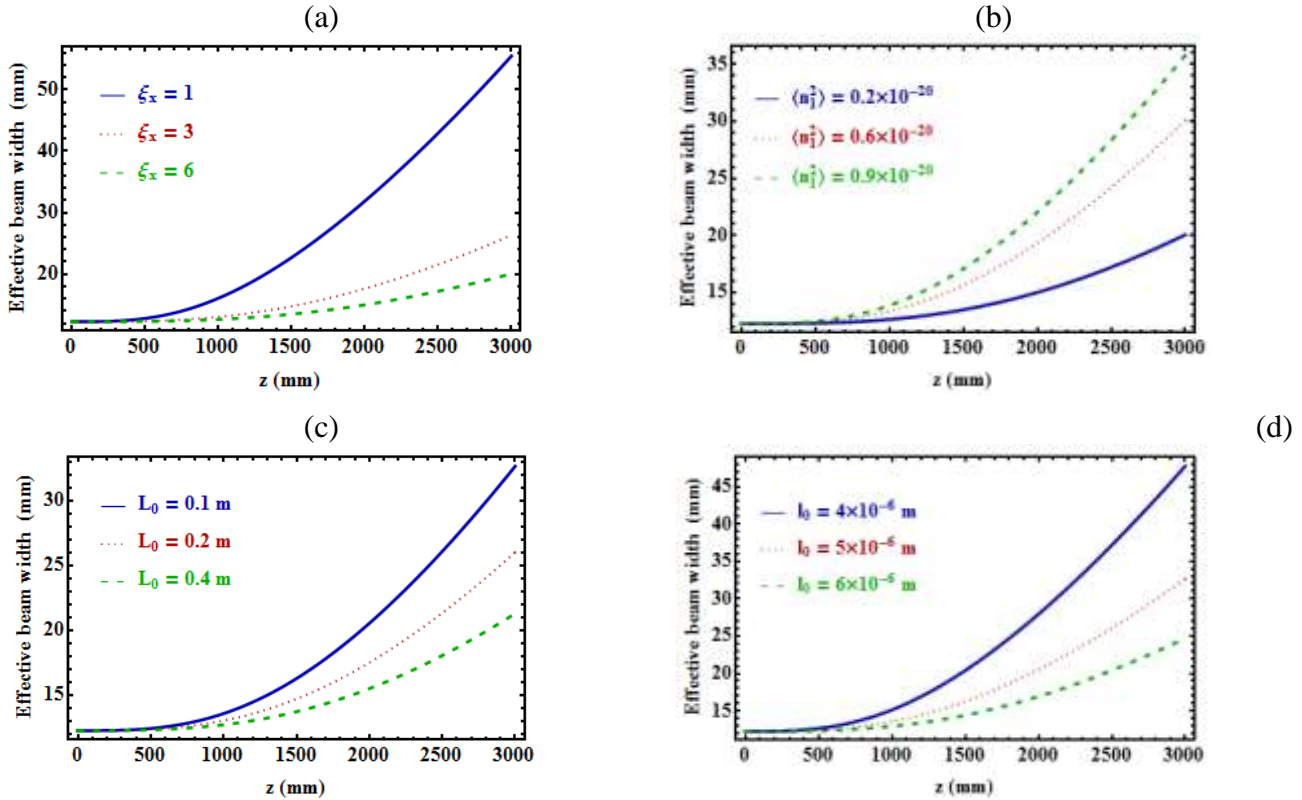


Figure 3 : Effective beam width of the partially coherent RMGSM vortex beam versus the propagation distance z in the turbulent plasma for the different : (a) anisotropy parameter ξ_x , (b) refractive index fluctuation variance $\langle n_1^2 \rangle$, (c) outer scale L_0 , and (d) inner scale l_0 .

The results shown in the previous figures are owing to the partially coherent vortex beam being impacted by turbulence and diffraction as it propagates. The diffraction effect predominates early in the passage of the vortex beam. The effect of turbulence became more prominent as the propagation distance of the

vortex beam increased in the anisotropic turbulent plasma, which spread the beam spot.

4. Conclusion

In this study, based on the extended Huygens-Fresnel integral, analytical expressions for the optical intensity and effective beam width of a partially coherent RMGSM vortex beam

propagating through anisotropic turbulent plasma is derived and used to study the evolution of the effective beam width using numerical examples. The results indicate that the partially coherent RMGSM vortex beam propagating through turbulent plasma loses its central dark core and transforms into a beam that resembles a Gaussian as the propagation distance z increases. We also found that the effective beam widths in the x - and y -directions are similar. The source parameters l , σ , and w_0 affect the effective beam width of a partially coherent RMGSM vortex beam in turbulent plasma. The effective beam width was relatively larger for larger parameters l and w_0 , and σ was smaller for the source. The effect of $N_1 = N_2$ on the effective beam width can be disregarded. In addition, the numerical results demonstrate that the effective beam width increases with the propagation distance, and a partially coherent RMGSM vortex beam propagating in turbulent plasma with smaller ξ_x , L_0 , and l_0 or larger $\langle n_1^2 \rangle$ will have a larger effective beam width.

* **Disclosures:**

The authors declare no conflicts in interest

References

- [1] S. Wang and M. Plonus, "Optical beam propagation for a partially coherent source in the turbulent atmosphere", *JOSA*, 69(9): 1297-1304,1979, <https://doi.org/10.1364/JOSA.69.001297>.
- [2] J. C. Ricklin and F. M. Davidson, "Atmospheric turbulence effects on a partially coherent Gaussian beam: implications for free-space laser communication", *JOSA A*, 19(9): 1794-1802,2002, <https://doi.org/10.1364/JOSAA.19.001794>.
- [3] T. Lin and L. Sproul, "Influence of reentry turbulent plasma fluctuation on EM wave propagation", *Computers & fluids*, 35(7): 703-711,2006, <https://doi.org/10.1016/j.compfluid.2006.01.009>.
- [4] H. Ding, S. Yi, Y. Zhu, et al., "Experimental investigation on aero-optics of supersonic turbulent boundary layers", *Applied Optics*, 56(27): 7604-7610,2017, <https://doi.org/10.1364/AO.56.007604>.
- [5] R. P. Starkey, "Hypersonic vehicle telemetry blackout analysis", *Journal of Spacecraft and Rockets*, 52(2): 426-438,2015, <https://doi.org/10.2514/1.A32051>.
- [6] C. Lv, Z. Cui and Y. Han, "Light propagation characteristics of turbulent plasma sheath surrounding the hypersonic aircraft", *Chinese Physics B*, 28(7): 074203,2019, <https://doi.org/10.1088/1674-1056/28/7/074203>.
- [7] J. Li, S. Yang and L. Guo, "Propagation characteristics of Gaussian beams in plasma sheath turbulence", *IET Microwaves, Antennas & Propagation*, 11(2): 280-286,2017, <https://doi.org/10.1049/iet-map.2016.0352>.
- [8] J. Li, J. Li, L. Guo, et al., "Polarization characteristics of radially polarized partially coherent vortex beam in anisotropic plasma turbulence", *Waves in Random and Complex Media*, 31(6): 1931-1944,2021, <https://doi.org/10.1080/17455030.2020.1713421>.
- [9] A. A. Alkelly, M. A. H. Khaled and L. F. Hassan, "Propagation of Partially Coherent Flat-Topped Vortex Hollow Beams in Anisotropic Turbulent Plasma", *International Journal of Optics*, 2022(7798053),2022, <https://doi.org/10.1155/2022/7798053>.
- [10] A. A. Alkelly, M. Khaled and L. F. Hassan, "Influence of anisotropic turbulent plasma on the partially coherent Four-petal Gaussian vortex beams", *Electronic Journal of University of Aden for Basic and Applied Sciences*, 3(3): 145-151,2022, <https://doi.org/10.47372/ejua-ba.2022.3.179>.
- [11] A. A. Alkelly, M. Khaled and L. F. Hassan, "Spreading properties of partially coherent multi-Gaussian Schell-model and modified Bessel-correlated vortex beams in anisotropic turbulent plasma", *Physica Scripta*, 98(7): 2023, <https://doi.org/10.1088/1402-4896/acdf90>.
- [12] G. Gbur and R. K. Tyson, "Vortex beam propagation through atmospheric turbulence and topological charge conservation", *JOSA A*, 25(1): 225-230,2008, <https://doi.org/10.1364/JOSAA.25.000225>.
- [13] T. Wang, J. Pu and Z. Chen, "Propagation of partially coherent vortex beams in a turbulent atmosphere", *Optical Engineering*, 47(3): 036002-036005,2008, <https://doi.org/10.1117/1.2896309>.
- [14] Y. Song, Y. Dong, S. Chang, et al., "Model of a rectangular multi-Gaussian Schell-model vortex beam and its properties", *Optik*, 192(162962),2019, <https://doi.org/10.1016/j.ijleo.2019.162962>.
- [15] Y. Dong, K. Dong, S. Chang, et al., "Propagation of rectangular multi-Gaussian Schell-model vortex beams in turbulent atmosphere", *Optik*, 207(163809),2020, <https://doi.org/10.1016/j.ijleo.2019.163809>.
- [16] W. H. Carter, "Spot size and divergence for Hermite Gaussian beams of any order", *Applied Optics*, 19(7): 1027-1029,1980, <https://doi.org/10.1364/AO.19.001027>.

- [17] L. C. Andrews and R. L. Phillips, "Laser beam propagation through random media : 2nd", *SPIE Publications* 2005,
- [18] G. Gbur and E. Wolf, "Spreading of partially coherent beams in random media", *JOSA A*, 19(8): 1592-1598,2002,
<https://doi.org/10.1364/JOSAA.19.001592>.
- [19] J. Li, S. Yang, L. Guo, et al., "Anisotropic power spectrum of refractive-index fluctuation in hypersonic turbulence", *Applied Optics*, 55(32): 9137-9144,2016,
<https://doi.org/10.1364/AO.55.009137>.
- [20] A. Jeffrey and H. H. Dai, "Handbook of mathematical formulas and integrals : 4th", *Elsevier* 2008.
- [21] I. S. Gradshteyn and I. M. Ryzhik, "Table of integrals, series, and products : 7th", *Elsevier* 2007.